Asian Journal of Chemistry; Vol. 34, No. 12 (2022), 3162-3168

ASIAN JOURNAL OF CHEMISTRY

https://doi.org/10.14233/ajchem.2022.24031

Adsorptive and Anticorrosive Studies of Guar Gum and Halides with Mild Steel in Acidic Medium

HIMANSHU SHEKHAR SHUKLA[1,*], RAJEEV PRADHAN[1], G. UDAYBHANU[2] and TRIVENI KUMAR MAHTO[1]

[1]Department of Chemistry, P.K. Roy Memorial College (Affilated to Binod Bihari Mahto Koyalanchal University), Dhanbad-826004, India
[2]Department of Applied Chemistry, Indian Institute of Technology (Indian School of Mines), Dhanbad-826004, India

*Corresponding author: E-mail: ismhs_shukla@yahoo.com

Received: 2 July 2022; *Accepted*: 17 September 2022; *Published online*: 25 November 2022; AJC-21041

The inhibitory effect of guar gum (GG) as a green inhibitor has been studied using a variety of methodologies, including weight loss, thermometric studies at 30-60 ºC. The potentiodynamic polarization, electrochemical impedance spectroscopy (EIS) and scanning electron micrographs have been found to the good inhibitor for mild steel corrosion in H_2SO_4 (pH = 1) medium. Guar gum fits to the Langmuir adsorption isotherm when it adsorbs to metal surfaces. It has also been investigated how adding halides (KCl, KBr and KI) will affect the process. The findings demonstrated that guar gum concentration increased with inhibition efficiency (I%). All of the concentrations of guar gum are shown to be promoted by the inhibitive impact of guar gum in addition to halide ions. The trend $Cl^- < Br^- < I^-$ has been seen to improve inhibition efficiency (I%) and the extent of surface coverage (θ), which suggests that the electronegativity and radii of the halide ions play a significant role in the adsorption process. According to polarization curves, guar gum functions as a mixed-type inhibitor. The outcomes of gravimetric studies and electrochemical procedures were in good agreement. Based on thermodynamic characteristics and a comparison of the FT-IR spectra of pure and metal surface product, a thorough adsorption of the inhibitor molecules on the mild steel surface was proposed. When the synergism parameter (S_I) was analyzed, it is found to be greater than unity, indicating that synergism alone is responsible for the increased inhibitory efficiency caused by the addition of halides.

Keywords: Mild steel, Guar gum, Adsorption, Anticorrosive, FTIR, Micrographs.

INTRODUCTION

Due to its low cost and great mechanical strength, mild steel is one of the metals that is most frequently employed in industries. However, mild steel corrodes easily and its rate of corrosion is fairly high in an acidic environment, meaning that the life of this valuable metal must be maintained during industrial acid treatment processes such as acid cleaning, pickling, *etc*. [1-3]. Among the several corrosion prevention techniques, applying inhibitors is one of the most practical because it doesn't interfere with the industrial process [4,5]. Numerous inhibitors have either been synthesized or chosen from organic compounds with hetero atoms in their chemical structures due to their industrial usefulness [6,7]. Additionally, there has been an increase in studies into the utilization of naturally occurring chemicals [8]. Several toxic, expensive manmade chemicals and inorganic substances are found in nature [9]. Thus, it is crucial to pick corrosion inhibitors that are affordable and easy to handle. Recent investigations by electrochemists and corrosion researchers opt for organic compounds, which are naturally occurring or biodegradable that could be employed as green inhibitors. Natural occurring polymers are a class of organic molecules that, due to their availability in nature and affordability, meet the majority of requirements for such a purpose [10]. In acidic medium, synergistic inhibition is a useful technique for increasing the potency of individual inhibitors, reducing their dosage and expanding the range of applications [11,12]. Several studies [13,14] have conducted indepth study on the synergism between organic inhibitors and halide ions in preventing steel corrosion in acidic solutions.

Natural materials are a cheap, environmentally begnin and completely safe source of materials that are also easily accessible and renewable. Acacia gum, guar gum, gum tragacanth, natural honey [15,16], henna, jojoba oil, artemisia oil and *Telferia occidentalis* extract [17], to name a few, have all been found to be very effective corrosion inhibitors for mild steel

in acidic medium. However, it has been observed that adding halide salts to acid solutions containing any organic components has a synergistic effect which prevents the iron corrosion. Increased surface coverage brought on by ion-pair interactions between the organic cations and the anions lead to synergistic corrosion inhibition. Synthetic polymers and halide ions are frequently used to suppress corrosion [18,19], but less is known about how halide ions interact with naturally occurring polymers to do the same.

Chemically, guar gum is a polysaccharide composed of the sugars galactose and mannose. The backbone is a linear chain of β-1,4-linked mannose residues to which galactose residues are 1,6-linked at every second mannose, forming short side branches (Fig. 1). Guargumisa naturally occurring polysaccharide consisting of D-mannopyranose and D-galactopyranose units joined to every other mannose unit has multiple adsorption sites for bonding with the metal surface through oxygen atoms. The complex structures of guar gum show good corrosion inhibitors due to its biodegradability, cost effective, easy availability, non-toxic, environment friendly properties. Verma *et al.* [20] concluded that the cyclic rings, odd atoms and π-electron densities present in the structure increase the efficiency, allowing them on to deposit above the metal surface.

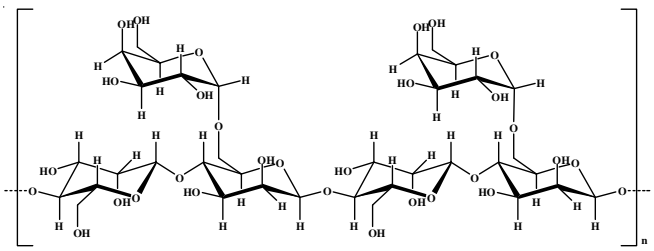

Fig. 1. Structure of guar gum (GG)

In present work, guar gum (GG) has been investigated as a mild steel corrosion inhibitor in H_2SO_4 solution (pH = 1). The variations in corrosion rate as a function of time, inhibitor concentration and temperature has been studied. The synergistic effects of halides with guar gum have been identified at various amount and exposure times. With the help of FTIR spectroscopy, the metal surface product has been examined to understand better of the inhibitory process. SEM technique has been used to study the surface morphology of the metal surface before and after corrosion in the absence and presence of inhibitors. A plausible adsorption mechanism for the inhibitor molecules adhering to the metal surface in acid solution has also been proposed.

EXPERIMENTAL

Under various experimental conditions, experiments were conducted to study the inhibitory behaviour of guar gum against corrosion on mild steel in H_2SO_4 (pH = 1). To ascertain the corrosion parameters, gravimetric analysis, potentiodynamic polarization and AC impedance measurements were performed at various temperatures (303, 313, 323 and 333 K) and exposure times (6, 12 and 24 h) both in the absence and presence of inhibitors at various concentrations (10, 50, 75, 100, 150, 200, and 300 ppm). With the ideal concentration of guar gum, the synergistic effect of halides (KCl, KBr and KI) has been investigated at various exposure times and temperatures. A mild steel sample from the investigation was analyzed and the results are shown in Table-1.

The mild steel sheets were used to cut the steel coupons in size of 4.4 cm × 2.2 cm × 0.15 cm, with a small hole measuring about 1 mm in diameter at the upper edge of specimen. The steel coupons' surface was mechanically abraded to clean it and then polished with progressively finer emery paper grades to eliminate the scratches. Following polishing, these were cleaned, degreased with acetone, washed and then dried in a warm air stream. Analytical grade H_2SO_4 provided by Ranbaxy Fine Chemicals was used to prepare a H_2SO_4 (pH = 1) test solution in distilled water. Sulphuric acid (pH = 1) was utilized in 500 mL for the immersion test and 250 mL for the electrochemical studies. The potentiodynamic polarization curves were measured using a potentiostat at room temperature (25 to 30 ºC) using mild steel as the working electrode in the absence and presence of inhibitors at various concentrations. The experimental methodologies for the aforementioned study are described in more detail elsewhere [21-24].

RESULTS AND DISCUSSION

The effect of concentration on inhibition efficiency of the inhibitors has been studied at 6 h immersion period at room temperature. As can be seen in Fig. 2, the inhibition efficacy rises with increasing inhibitor concentrations up to 250 ppm (79.04%) before tending to a constant value. The inhibition efficiency of guar gum has been found at 46.52% at 10 ppm. The degree of surface coverage (θ) was tested graphically for fitting a suitable adsorption isotherm and best fit was Langmuir adsorption isotherm shown in Fig. 3.

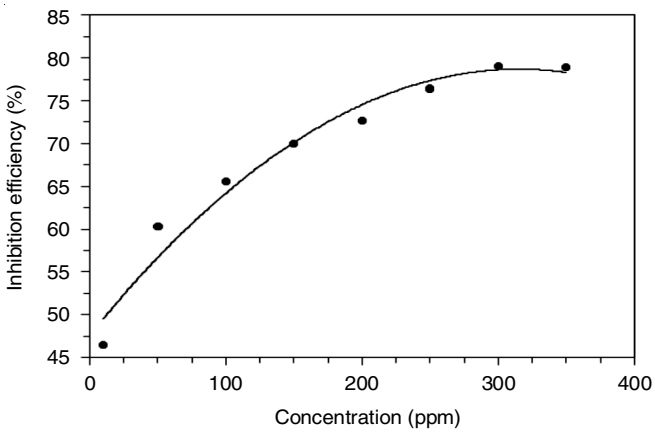

Fig. 2. Variation of inhibition efficiency with the inhibitor concentration

TABLE-1
COMPOSITION OF THE MILD STEEL COUPONS

C (%)	S (%)	P (%)	Si (%)	Al (%)	Mn (%)	W (%)	Fe (%)
0.12	0.02	0.01	0.15	0.01	0.57	0.015	Rest

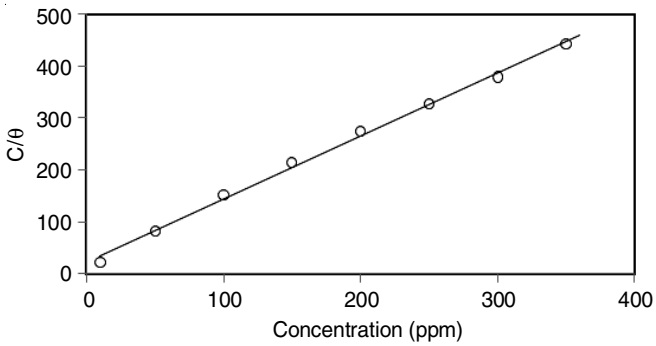

Fig. 3. Variation of c/θ with concentration of C

The corrosion parameters for both single applications of guar gum and for combinations with halides are listed in Table-2. The inhibitive impact of guar gum was found to be promoted at all guar gum concentrations containing halide ions (Table-2).

When 250 ppm guar gum was mixed with 700 ppm iodide, the highest efficiency (92%) was attained. It is well known that in acidic medium, halide ions make it easier for organic inhibitors to bind to metal surfaces through intermediary bridges with positively charged inhibitors. Therefore, the presence of the halide ions should result in a synergistic increase in inhibitory efficiency [25,26]. According to reports [27,28], the synergistic impact grows in the following order: $I^- > Br^- > Cl^-$. Iodide ions have a higher synergistic effect than other anions due to their wide ionic radius, strong hydrophobicity and low electronegativity. Efficiency of inhibition was attained in the following order:

GG + Iodide > GG + Bromide > GG + Chloride > GG

The corrosion rate and percentage inhibition were investigated at the optimum inhibitor concentration and 700 ppm halides, it was revealed that the corrosion rate for free acid increased with exposure time while the corrosion rate for inhibited acid decreased with exposure time of 24 h (Fig. 4). This is happened, since an increase in temperature typically speeds up corrosion processes, especially in acid media where H_2 gas evolution occurs.

The inhibition efficiency of corrosion decreased with temperature at optimum concentration of the inhibitors (Fig. 5). It has been found that corrosion rate increases with the increase in temperature and the inhibition efficiency offered by GG, GG + Cl^-, GG + Br^- and GG + I^- was 70.56%, 78.43%, 78.78% and 81.47% at 333 K respectively, it may be because

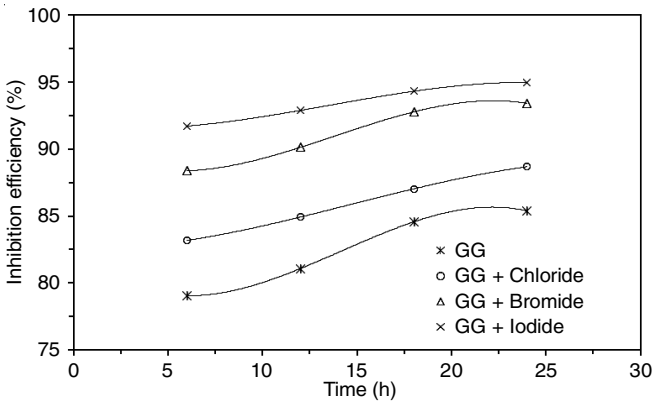

Fig. 4. Variation of inhibition efficiency in presence of the GG and GG + halides at different exposure period

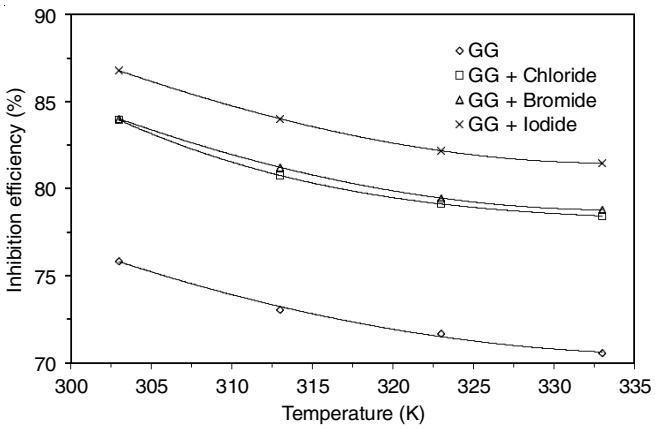

Fig. 5. Variation of inhibition efficiency in presence of the GG and GG + halides at different temperature

of at higher temperature accelerates desorption of guar gum from the mild steel surface.

The thermodynamic parameters in absence and in presence of the inhibitors have been calculated from the well-known equations and are given in Table-3. The E_a value has been calculated ~ 44 kJ/mol, indicates the formation of an adsorptive film of a physical electrostatic character. The negative values of ΔG_{ads} ensure the spontaneity of the adsorption process on the mild steel surface [29,30]. The ΔG_{ads} values, which were less than - 20 kJ/mol, indicated that guar gum physically reacted with the surface of mild steel. The exothermic and physical adsorption of the inhibitors on the metal surface, which makes the dissolution of steel challenging, was demonstrated by the

TABLE-2
CORROSION PARAMETERS IN PRESENCE OF GUAR GUM AND GG + HALIDES AT DIFFERENT CONCENTRATIONS

Concentration (ppm)				CR (mpy)	IE (%)	Surface coverage (θ)	s
Gum gum	Chloride	Bromide	Iodide				
0	0	0	0	359.70	–	–	–
100	0	0	0	107.98	69.98	0.6998	
100	700	0	0	88.31	75.45	0.7545	2.12
100	0	700	0	84.71	76.45	0.7645	1.46
100	0	0	700	59.78	83.38	0.8338	1.12
250	0	0	0	75.39	79..04	0.7904	–
250	700	0	0	60.54	83.17	0.8317	2.53
250	0	700	0	41.83	88.37	0.8837	2.08
250	0	0	700	29.78	91.72	0.9172	1.13

TABLE-3
THERMODYNAMIC PARAMETERS IN ABSENCE AND IN PRESENCE GUAR GUM AND GG + HALIDES

Parameters (kJ/mol)	Blank	Guar gum	GG + chloride (250 + 700) ppm	GG + bromide (250 + 700) ppm	GG + iodide (250 + 700) ppm
Heat of adsorption	–	-47.121	-49.859	-49.629	-51.161
Activation energy	44.306	49.763	52.501	52.272	53.784
Average free energy	–	-7.460	-10.098	-9.775	-11.259
Entropy of adsorption	–	0.048	0.041	0.042	0.039

negative values of ΔH_{ads}. Positive ΔS_{ads} values for inhibitors may be the result of inhibitor molecules replacing the water molecules, which were initially adsorbed on the metal surface since the inhibitor molecules have a higher affinity to the metal surface than water does [29]. The polymer makes the adsorption process entropically favourable by displacing water molecules from the metal surface, while the several bonding sites slow down the desorption process [31]. The potential dynamic parameters for corrosion of the mild steel in the acid containing pure guar gum and guar gum with the halides are summarized in Table-4.

Higher concentration levels showed a considerable decrease in corrosion current (I_{corr}), indicating increased inhibitor adsorption and improved inhibition efficacy (Fig. 6a-b). When these inhibitors were present, variations in the levels of both Tafel slopes were observed indicating the mixed inhibition [32]. No distinct change in the cathodic current densities is caused by the inhibitor's presence in the corrosive medium. The potentiodynamic polarisation study's predicted inhibitory efficiencies and those from the weight loss trial differed marginally. The reason for this is that unlike long-term research like weight loss experiments, potentiodynamic polarization analysis are conducted for a brief period of time and operate on a different principle.

The electrochemical parameters for corrosion of the mild steel in the acid containing pure guar gum and guar gum with the halides are summarized in Table-5. The creation of a protective film at the metal-solution interface results in the increase of R_t values with the inhibitor concentration, which affects an increase in IE%. The impedance diagrams shown in Fig. 7a-b

TABLE-4
POTENTIAL DYNAMIC POLARIZATION PARAMETERS IN THE ABSENCE AND IN PRESENCE OF GUAR GUM AND GG + HALIDES

Concentration of inhibitor	E_0 (V)	I_0 (m amp/cm^2)	Tafel slopes (mV)		PI
			Anodic (b_a)	Cathodic (b_c)	
Blank	-0.5518	423.0	124.16	191.93	–
Guar gum					
50 ppm	-0.5389	157.4	96.25	168.58	62.78
100 ppm	-0.5403	137.1	87.94	174.76	67.59
250 ppm	-0.5318	99.59	70.98	172.21	76.46
GG + Chloride					
100 + 700 ppm	-0.5409	98.09	77.48	159.62	76.81
250 + 700 ppm	-0.5349	67.13	69.74	181.88	85.50
GG + Bromide					
100 + 700 ppm	-0.5397	91.63	77.63	169.12	78.33
250 + 700 ppm	-0.5458	44.31	82.10	109.30	89.60
GG + Iodide					
100 + 700 ppm	-0.5578	61.35	73.50	118.68	85.50
250 + 700 ppm	-0.5489	26.05	87.20	117.50	93.84

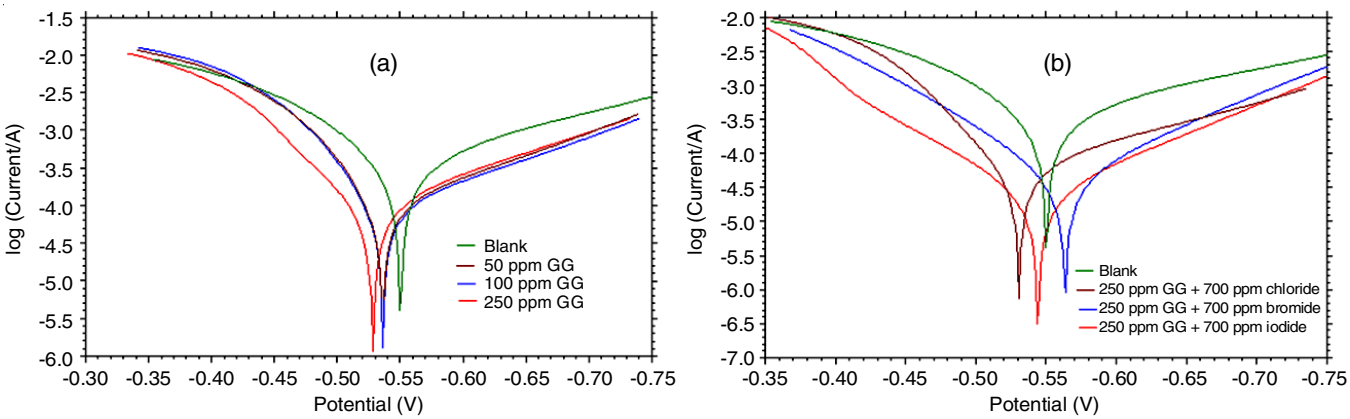

Fig. 6. Potentiodynamic polarization curves in absence and inpresence of (a) GG at different concentration and (b) GG and GG + halides concentration

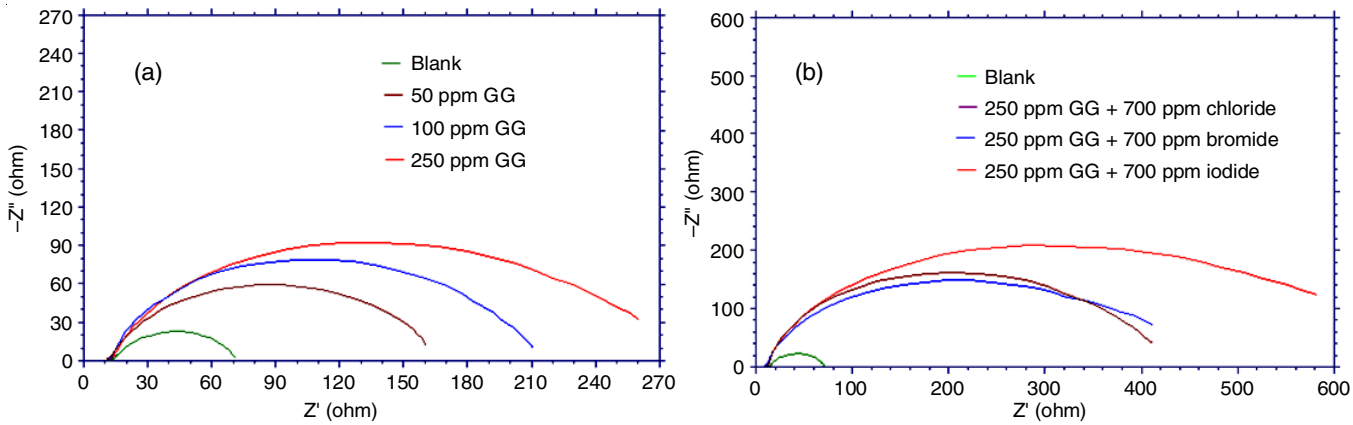

Fig. 7. Electrochemical (Nyquist) impedance plots in absence and in presence of (a) GG and (b) GG and GG + halides

TABLE-5
ELECTROCHEMICAL IMPEDANCE PARAMETERS
IN PRESENCE OF GUAR GUM AND GG + HALIDES

Inhibitor concentration	R_t (Ω cm^2)	C_{dl} (μF cm^{-2})	I.E. (%)
Blank	58	121.32	–
50 ppm GG	146	38.48	64.66
100 ppm GG	194	10.38	70.10
250 ppm GG	260	9.46	77.69
Blank	–	–	–
250 ppm GG + 700 ppm chloride	400	2.52	85.50
250 ppm GG + 700 ppm bromide	410	2.47	85.85
250 ppm GG + 700 ppm iodide	600	1.38	90.33

are suppressed semicircles with the real axis at the centre. This characteristic demonstrates the role played by surface roughness, the distribution of active sites, the adsorption of inhibitors, and the development of porous layers.

As can be seen from Table-5, values of double layer capacity (C_{dl}) in the case of guar gum tend to decrease as the concentration of the inhibitor increases. An increase in the electrical double layer's thickness can cause a decrease in C_{dl} values. According to this behaviour, inhibitor molecules work by adsorbing at the metal-solution contact. Similar trends have been observed when halides have been added. The lower dielectric constant organic inhibitor molecules that have been adsorbing at the electrode interface may have replaced the water molecules, resulting in the lowered values of double layer capacitance (C_{dl}).

Guar gum displayed the expected –OH bond bands at 3425 cm^{-1} and the metal surface obtained product at 3422 cm^{-1} (Fig. 8). Pure guar gum exhibits asymmetric and symmetric stretching vibrations of the carboxylic acid, which result in two strong bands at 1616 and 1423 cm^{-1}, respectively, which were observed at 1561 and 1401 cm^{-1} in the metal surface product [25-27]. The metal surface product displaced the band that was formed at 1042 cm^{-1} due to the stretching of the CO bond to 1023 cm^{-1}. The ring breathing peak for guar gum was achieved at 1641 cm^{-1}, however it changed to and at 1673 cm^{-1} for the metal surface product.

A SEM analysis showed that the mild steel surface was severely corroded without guar gum, with patches of uniform corrosion (Fig. 9b). However, when an inhibitor was present, the specimen surface became smoother (Fig. 9c–f) and the

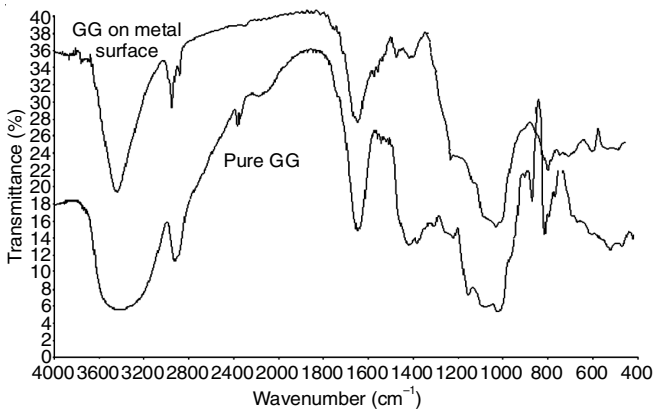

Fig. 8. FT-IR spectra of GG both as pure form and in metal surface product

quasi-globular inhibitor products partially covered the metal surface. This is because inhibitor molecules were involved in the interaction with the reaction sites on the mild steel surface, which reduced the amount of time that iron was in touch with the hostile medium and successively displayed outstanding inhibitory effect [33-36]. When guar gum, bromide and iodide are combined, a more compact layer is observed (Fig. 9e-f).

Conclusion

In this work, the combination of 250 ppm guar gum and 700 ppm iodide during a 6 h exposure time exhibited the highest inhibitory efficiency for the three combinations, with guar gum exhibiting maximum efficiency (79.04%) for the corrosion of mild steel in H_2SO_4 (pH = 1) medium. Higher synergism parameters have been achieved for both combinations (250 ppm guar gum and 700 ppm chloride/bromide). Guar gum adheres to the Langmuir adsorption isotherm when it is adsorbed to mild steel surfaces in sulphuric acid media. The negative ΔG_{ads} readings and smaller negative ΔH_{ads} values showed that guar gum physisorbed on the metal surface on its own. Lower ΔS_{ads} values were obtained, which might be related to the desorption of water molecules that inhibitor molecules had initially adsorbed on metal surfaces. A significant chemisorption of halide ions on the metal surface seems to cause the synergistic effect between guar gum and the halides, which was observed ($s > 1$). On the metal surface, where halide ions have previously been adsorbed through chemisorption, the inhibitors are subsequ-

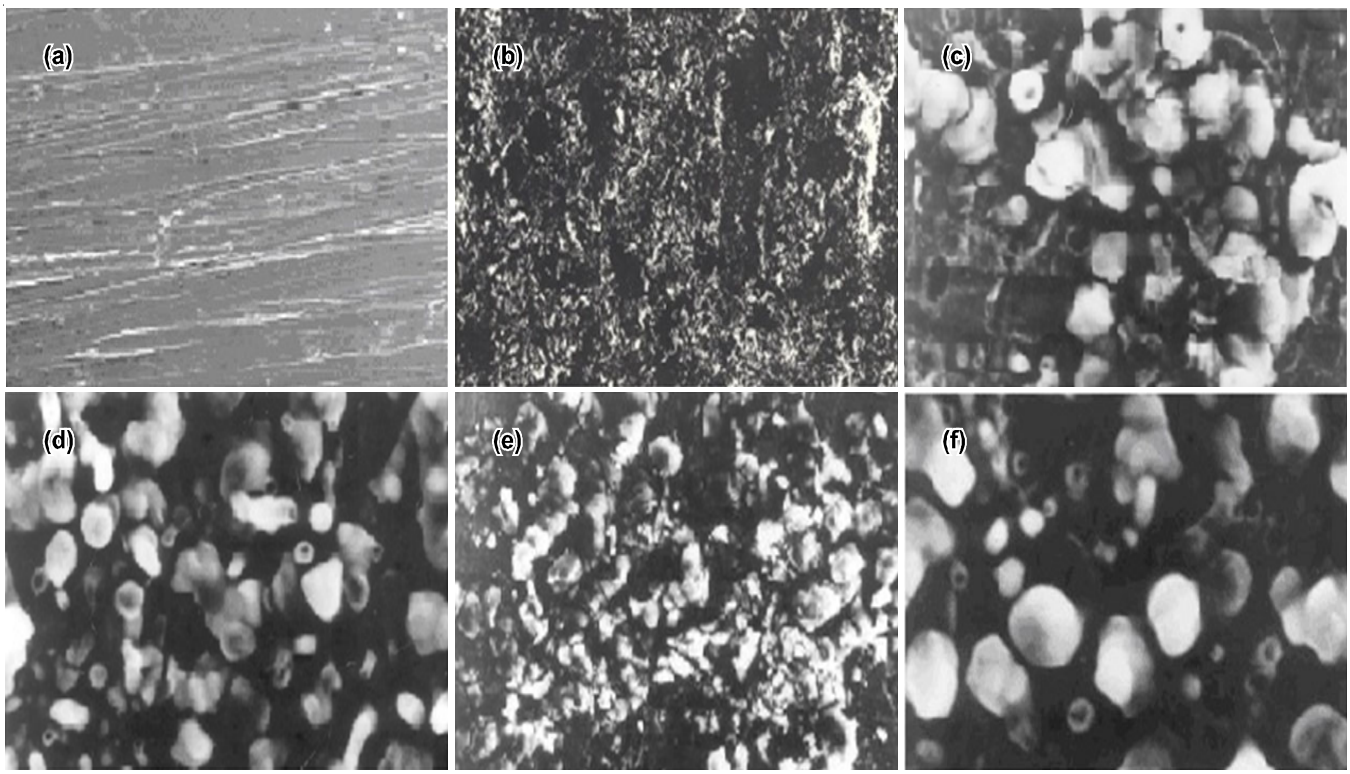

Fig. 9. SEM Micrographs of the metal surface at 3000X magnification in absence and in presence of the inhibitors (a) before exposure, (b) blank, (c) 250 ppm GG, (d) 250 ppm GG + 700 ppm chloride, (e) 250 ppm GG + 700 ppm bromide, (f) 250 ppm GG + 700 ppm iodide

ently adsorbed by coulombic attraction. The size and electronegativity of the halide ions may play a role in the inhibitory effectiveness of combinations that follow the trend of iodide > bromide > chloride. For pure guar gum and all guar gum and halide mixtures, the potentiodynamic analysis recommended mixed type inhibition and preferring cathodic control over anodic control. Guar gum was found in the metal surface product according to a comparative FT-IR analysis and a possible explanation for the modest variation in peak or band locations is the interaction of adsorbed inhibitor molecules with the metal surface. From SEM micrographs, it was possible to observe that the metal surface was partially covered with the inhibitor products as well as flake-type metal oxide and metal hydroxide deposition.

CONFLICT OF INTEREST

The authors declare that there is no conflict of interests regarding the publication of this article.

REFERENCES

1. J. Aljourani, M.A. Golozar and K. Raeissi, *Mater. Chem. Phys.*, **121**, 320 (2010); https://doi.org/10.1016/j.matchemphys.2010.01.040
2. O.S.I. Fayomi and A.P.I. Popoola, *J. Phys.: Conf. Ser.*, **1378**, 022006 (2019); https://doi.org/10.1088/1742-6596/1378/2/022006
3. M. Vankeerberghen, S. Gavrilov and G. Nelissen, *Corros. Sci.*, **43**, 37 (2001); https://doi.org/10.1016/S0010-938X(00)00072-X
4. M.J. Bahrami, S.M.A. Hosseini and P. Pilvar, *Corros. Sci.*, **52**, 2793 (2010); https://doi.org/10.1016/j.corsci.2010.04.024
5. P. Dohare, K.R. Ansari, M.A. Quraishi and I.B. Obot, *J. Ind. Eng. Chem.*, **52**, 197 (2017); https://doi.org/10.1016/j.jiec.2017.03.044
6. M. Goyal, S. Kumar, I. Bahadur, C. Verma and E.E. Ebenso, *J. Mol. Liq.*, **256**, 565 (2018); https://doi.org/10.1016/j.molliq.2018.02.045
7. L. Li, C. Tan, Y. Chen, W. Guo and F. Song, *Mater. Des.*, **43**, 59 (2013); https://doi.org/10.1016/j.matdes.2012.06.057
8. A. Kosari, M.H. Moayed, A. Davoodi, R. Parvizi, M. Momeni, H. Eshghi and H. Moradi, *Corros. Sci.*, **78**, 138 (2014); https://doi.org/10.1016/j.corsci.2013.09.009
9. H. Ali, E. Khan and I. Ilahi, *J. Chem.*, **2019**, 6730305 (2019); https://doi.org/10.1155/2019/6730305
10. K.R. Ansari and M.A. Quraishi, *J. Ind. Eng. Chem.*, **20**, 2819 (2014); https://doi.org/10.1016/j.jiec.2013.11.014
11. P.B. Matad, P.B. Mokshanatha, N. Hebbar, V.T. Venkatesha and H.C. Tandon, *Ind. Eng. Chem. Res.*, **53**, 8436 (2014); https://doi.org/10.1021/ie500232g
12. P. Rugmini Ammal, A.R. Prasad and A. Joseph, *Egypt. J. Petrol.*, **27**, 1067 (2018); https://doi.org/10.1016/j.ejpe.2018.03.006
13. J. Tan, L. Guo, H. Yang, F. Zhang and Y. El Bakri, *RSC Adv.*, **10**, 15163 (2020); https://doi.org/10.1039/D0RA02011G
14. M.P. Chakravarthy, K.N. Mohana and C.B. Pradeep Kumar, *Int. J. Ind. Chem.*, **5**, 19 (2014); https://doi.org/10.1007/s40090-014-0019-3
15. M.H. Hussin and M.J. Kassim, *Int. J. Electrochem. Sci.*, **6**, 1396 (2011).
16. M.H. Hussin, M. Jain Kassim, N.N. Razali, N.H. Dahon and D. Nasshorudin, *Arab. J. Chem.*, **9**, 5616 (2016); https://doi.org/10.1016/j.arabjc.2011.07.002
17. M.A.M. El-Haddad, A.B. Radwan, M.H. Sliem, W.M.I. Hassan and A.M. Abdullah, *Sci. Rep.*, **9**, 3695 (2019); https://doi.org/10.1038/s41598-019-40149-w
18. S.A. Umoren and M.M. Solomon, *Open Mater. Sci. J.*, **8**, 39 (2014); https://doi.org/10.2174/1874088X01408010039
19. R. Aslam, M. Mobin, J. Aslam and H. Lgaz, *Sci. Rep.*, **8**, 3690 (2018); https://doi.org/10.1038/s41598-018-21175-6

20. D.K. Verma, Y. Dewangan and A.K. Dewangan, *Mater. Res. Foundat.*, **107**, 70 (2021); https://doi.org/10.21741/9781644901496-4
21. M. Messali, H. Lgaz, R. Dassanayake, R. Salghi, S. Jodeh, N. Abidi and O. Hamed, *J. Mol. Struct.*, **1145**, 43 (2017); https://doi.org/10.1016/j.molstruc.2017.05.081
22. M. Basik, M. Mobin and M. Shoeb, *Sci. Rep.*, **10**, 279 (2020); https://doi.org/10.1038/s41598-019-57181-5
23. J. Fu, J. Pan, Z. Liu, S. Li and Y. Wang, *Int. J. Electrochem. Sci*., **6**, 2072 (2011).
24. S. Vishwanatham, N. Haldar, *Indian J. Chem. Technol.*, **14**, 501 (2007).
25. A. Popova, E. Sokolova, S. Raicheva and M. Christov, *Corros. Sci.*, **45**, 33 (2003); https://doi.org/10.1016/S0010-938X(02)00072-0
26. H. Ashassi-Sorkhabi and M. Es'haghi, *Mater. Chem. Phys.*, **114**, 267 (2009); https://doi.org/10.1016/j.matchemphys.2008.09.019
27. S.A. Umoren and M.M. Solomon, *Arab. J. Sci. Eng.*, **35**, 115 (2010).
28. S. Vishwanatham and N. Haldar, *Corros. Sci.*, **50**, 2999 (2008); https://doi.org/10.1016/j.corsci.2008.08.005
29. M.M. Singh and A. Gupta, *Bull. Electrochem.*, **12**, 511 (1996).
30. K.F. Khaled and N. Hackerman, *Electrochim. Acta*, **49**, 485 (2004); https://doi.org/10.1016/j.electacta.2003.09.005
31. M.P. Filippove, *Food Hydrocoll.*, **6**, 115 (1992); https://doi.org/10.1016/S0268-005X(09)80060-X
32. H. Espinosa-Andrews, O. Sandoval-Castilla, H. Vázquez-Torres, E.J. Vernon-Carter and C. Lobato-Calleros, *Carbohydr. Polym.*, **79**, 541 (2010); https://doi.org/10.1016/j.carbpol.2009.08.040
33. N.B. Colthup and L.H. Daly, Wiberley, Introduction to Infrared and Raman Spectroscopy, Ed. 3, Academic Press, Inc.: San Diego (1990).
34. K.F. Khaled and N. Hackerman, *Electrochim. Acta*, **48**, 2715 (2003); https://doi.org/10.1016/S0013-4686(03)00318-9
35. Z.A. Iofa and G.N. Tomasov, *Zh. Fiz. Khim.*, **34**, 1036 (1960).
36. S. Muralidharan, S. Syed Azim, L.J. Berchmans and S.V.K. Iyer, *Anti-corros. Met. Mater.*, **44**, 30 (1997); https://doi.org/10.1108/00035599710157378